



Deposited via The University of Sheffield.

White Rose Research Online URL for this paper:

<https://eprints.whiterose.ac.uk/id/eprint/129037/>

Version: Accepted Version

Article:

Chen, X., Jia, P., Wang, Y. et al. (2018) A surface-based approach to determine key spatial parameters of the acetabulum in a standardized pelvic coordinate system. *Medical Engineering and Physics*, 52. pp. 22-30. ISSN: 1350-4533

<https://doi.org/10.1016/j.medengphy.2017.11.009>

Reuse

This article is distributed under the terms of the Creative Commons Attribution-NonCommercial-NoDerivs (CC BY-NC-ND) licence. This licence only allows you to download this work and share it with others as long as you credit the authors, but you can't change the article in any way or use it commercially. More information and the full terms of the licence here: <https://creativecommons.org/licenses/>

Takedown

If you consider content in White Rose Research Online to be in breach of UK law, please notify us by emailing eprints@whiterose.ac.uk including the URL of the record and the reason for the withdrawal request.

1

> REPLACE THIS LINE WITH YOUR PAPER IDENTIFICATION NUMBER (DOUBLE-CLICK HERE TO EDIT)

<

A surface-based approach to determine key spatial parameters of the acetabulum in a standardized pelvic coordinate system

Xiaojun Chen ^{a,*}, Pengfei Jia ^a, Yiping Wang ^a, Henghui Zhang ^b, Liao Wang ^{b,*}, Zeike A. Taylor ^c, and Alejandro F. Frangi ^c

^a Institute of Biomedical Manufacturing and Life Quality Engineering, School of Mechanical Engineering, Shanghai Jiaotong University, Shanghai, China

^b Shanghai Key Laboratory of Orthopaedic Implants, Department of Orthopaedics, Shanghai Nine People's Hospital Affiliated to Shanghai Jiao Tong University School of Medicine, Shanghai, China

^c Center for Computational Imaging and Simulation Technologies in Biomedicine, The University of Sheffield, S1 3JD, Sheffield, UK

1 *Address correspondence to:

2

3 1. Xiaojun Chen, PhD
4 Room 805, School of Mechanical Engineering, Shanghai Jiao Tong University, Dongchuan Road 800,
5 Minhang District, Shanghai, China
6 Post Code: 200240
7 E-mail: xiaojunchen@163.com
8 Tel: (+86) -13472889728, (+86) 21-62816517
9 Fax: (+86)21-34206847

10

11 2. Liao Wang, MD
12 Department of Orthopaedics, Shanghai Nine People's Hospital Affiliated to Shanghai Jiao Tong University
13 School of Medicine, Zhizaoju Road 639, Huangpu District, Shanghai, China
14 Post Code: 200011
15 E-mail: wang821127@163.com
16 Tel: (+86)13564737682

17

18

19

20

Abstract

21 Accurately determining the spatial relationship between the pelvis and acetabulum is challenging due to their
22 inherently complex three-dimensional (3D) anatomy. A standardized 3D pelvic coordinate system (PCS) and the precise
23 assessment of acetabular orientation would enable the relationship to be determined. We present a surface-based method to
24 establish a reliable PCS and develop software for semi-automatic measurement of acetabular spatial parameters. Vertices
25 on the acetabular rim were manually extracted as an eigenpoint set after 3D models were imported into the software. A
26 reliable PCS consisting of the anterior pelvic plane, midsagittal pelvic plane, and transverse pelvic plane was then
27 computed by iteration on mesh data. A spatial circle was fitted as a succinct description of the acetabular rim. Finally, a
28 series of mutual spatial parameters between the pelvis and acetabulum were determined semi-automatically, including the
29 center of rotation, radius, and acetabular orientation. Pelvic models were reconstructed based on high-resolution computed
30 tomography images. Inter- and intra-rater correlations for measurements of mutual spatial parameters were almost perfect,
31 showing our method affords very reproducible measurements. The approach will thus be useful for analyzing anatomic
32 data and has potential applications for preoperative planning in individuals receiving total hip arthroplasty.

33 **Key words:** surface-based, acetabulum, pelvic coordinate system, total hip arthroplasty, computer assisted
34 surgery

35

36

1. Introduction

37 Total hip arthroplasty (THA) is considered to be a successful treatment for patients with end-stage hip osteoarthritis
38 [1]. Diseases and surgical procedures of the hip are inherently three-dimensional (3D), occurring in and around the
39 proximal femur and the acetabulum. With the advent of cementless implants, the orientation of the femoral component
40 must be consistent with the geometry of the femoral medullary cavity. Correct implantation of the acetabular component in
41 THA is critical with respect to long-term survival as well as short-term complications [2].

42 Lewinnek *et al.* [3] proposed a safe zone for the placement of the acetabular component based on radiological
43 analysis of the dislocation rates among 300 THAs. They recommended two related two-dimensional (2D) parameters for
44 defining the safe zone, including an inclination of 40° (standard deviation [SD] 10°) and an anteversion of 15° (SD 10°)

45 relative to the anterior pelvic plane (APP). This so-called safe zone is widely applied to guide the placement of the
46 acetabular component, although the ranges for the inclination and anteversion remain unknown. The native orientation of
47 the acetabulum or the transverse acetabular ligament [4] have also been used as guides, with satisfactory outcomes.
48 However, the complex 3D geometry of the anatomic landmarks makes the determination and description of their
49 orientations difficult [5, 6], especially when the mutual relationship of the acetabulum and pelvis is considered. These
50 complex anatomic structures do not allow for accurate measurement of their 3D orientations based on the 2D images
51 provided by radiography or traditional axial tomography [7-13]. In addition to the orientation [14, 15] of the acetabulum,
52 other mutual spatial parameters, such as the center of rotation, remain unknown, despite their importance for successful hip
53 joint reconstruction and the restoration of hip biomechanics [16]. Knowledge of these parameters will also benefit further
54 biomechanical and anatomical research.

55 To further clarify the spatial relationship between the acetabulum and pelvis, and especially the acetabular orientation,
56 a reliable pelvic coordinate system (PCS) is required [15, 17-21]. A reliable PCS consisting of the APP, midsagittal pelvic
57 plane (MSP), and transverse pelvic plane (TPP) is very important for the successful alignment of the acetabular component.
58 The APP, a plane defined by the bilateral anterior superior iliac spines (ASIS) and the midpoint between the bilateral pubic
59 tubercles, has the potential to be used to establish a reliable PCS. However, manual selection of these anatomic landmarks
60 does not reliably define the APP. A surface-based approach has been proposed in [22, 23] to overcome this drawback. By
61 manually selecting both ASISs and pubic tubercles on partly homologous surface patches, the APP can be reliably
62 computed by an iterative algorithm. The MSP and TPP can also be computed as the mirror plane associated with both
63 ASIS regions by using an iterative closest point (ICP) algorithm. We hypothesize that a reliable PCS can be established
64 from the APP, MSP, and TPP. Semi-automatically selected points on the osseous ridge of the acetabulum have been used
65 to generate a best-fit circle for describing acetabular orientation [24]. Here we describe a novel method to measure the 3D
66 acetabular orientation and center of rotation relative to the new PCS. The proposed method was recently used to study
67 acetabular orientation statistics within a cohort of Chinese subjects [25]. In the present contribution, we describe in detail
68 the technical aspects of the method, and investigate the intra- and inter-observer consistency of its results.

70 **2. Methods**

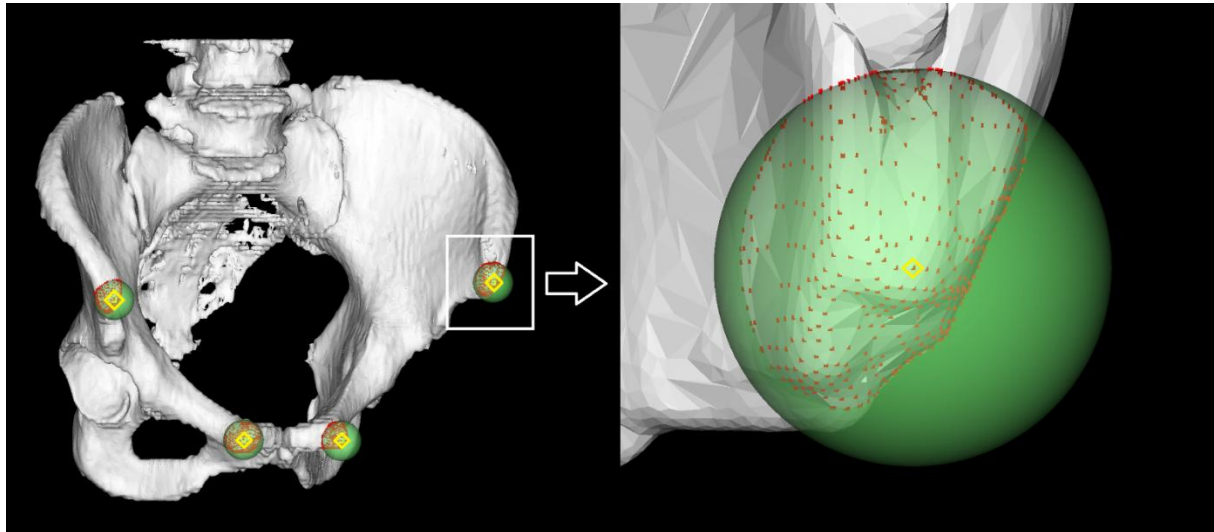
71 In this study, we present a unique algorithm to analyze various parameters related to the acetabulum, and a 3D
72 software implementation of the same. The processing and image rendering tools of the software are based on the
73 open-source libraries Insight Toolkit (ITK) and Visualization Toolkit (VTK). Surface models are reconstructed from
74 computed tomography (CT) data volumes through the threshold and region-growing segmentation method using 3D Slicer
75 4.2 (Surgical Planning Laboratory, Brigham and Women's Hospital, Harvard Medical School, United States,
76 <http://www.slicer.org/>). After reconstruction, 3D models of the acetabulum are imported into our software. By manually
77 selecting some anatomic landmarks on the model, the software can automatically calculate acetabular spatial parameters.
78 The entire acetabular rim, less the notch, is required to determine the actual 3D orientation of the acetabulum's aperture.
79 To achieve this, a 3D PCS needs to be established before acetabular measurements.

80 **2.1 Standardized pelvic coordinate system**

81 Four initial markers are manually located on the anatomical landmarks to begin the analysis (Fig. 1). Spheres with
82 centers at each initial marker are used to clip points on the surface model. The spherical implicit function F for clipping is

83
$$F = \overline{OP}^2 - R^2, \quad (1)$$

84 where $P \in U_{pelvis}$ is a point on the surface model U_{pelvis} ; R is the radius of the sphere, which should be large enough to
85 cover the landmark; and \overline{OP} is the distance between P and the sphere center O . Thus, four clipped point sets are used
86 in the APP and MSP computations.



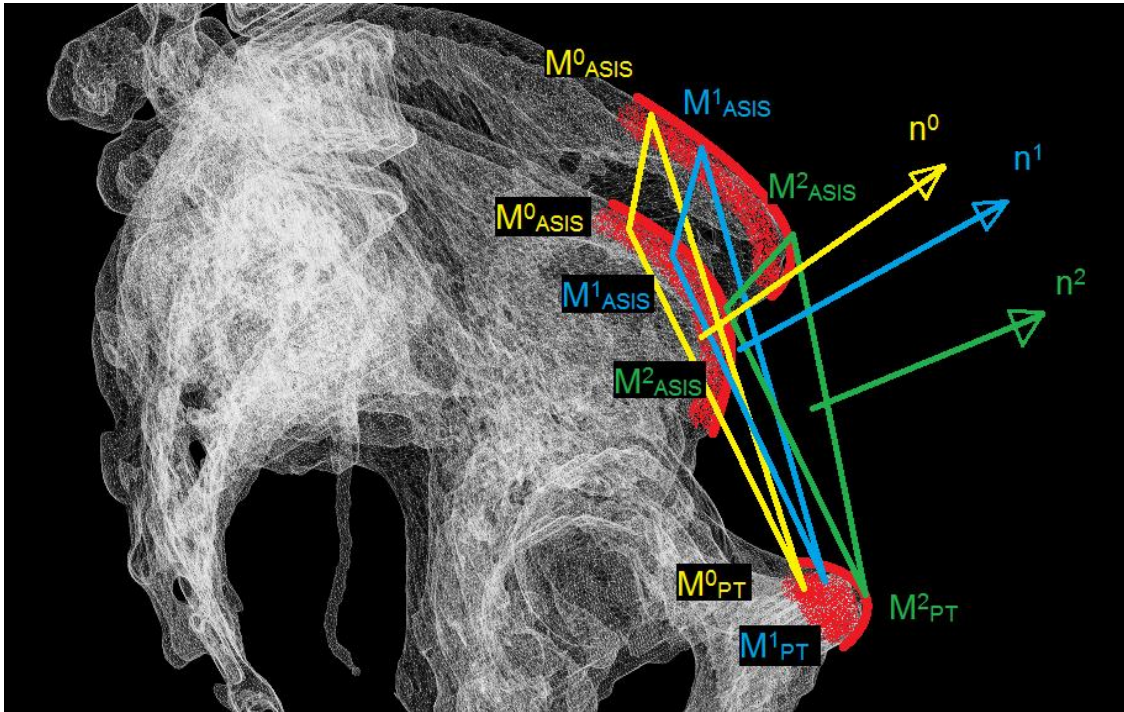
87

88 Fig. 1. Clipping landmark point sets on the pelvic surface. Four initial markers (yellow) are manually defined at positions near the landmarks.
 89 Point sets (red) are clipped using a spherical implicit function (green region; see equation (1)).

90 **2.1.1 Anterior pelvic plane**

91 The APP can be considered as a tangent plane containing the ASISs and the pubic tubercles. The initial APP consists
 92 of the initial ASIS marker bilaterally and the midpoint between the markers on the left and right pubic tubercles. At each
 93 step of the iteration, points in the clipped point set are sorted by their displacement relative to the APP determined by the
 94 current markers. The most anterior point becomes the next marker, and the APP is recomputed (Fig. 2). The algorithm will
 95 converge on a solution after several iterations. The general computation process can be described by the following steps:

<



96

97 Fig. 2. Schematic diagram of the APP iteration. Automatically searching the most anterior point on the landmarks (red), markers are modified
 98 from M^0 to M^2 (yellow \rightarrow blue \rightarrow green) within a few steps. The corresponding normal vector of the APP changes from n_0 to n_2 .

99 1. Manually locate initial markers M_i^0 (i is left ASIS, right ASIS, left pubic tubercle, or right pubic tubercle).

100 2. For markers M_i^k , compute the midpoint M_{mid}^k between pubic tubercles and create a plane APP^k with normal
 101 vector n^k defined by bilateral M_{ASIS}^k and M_{mid}^k .

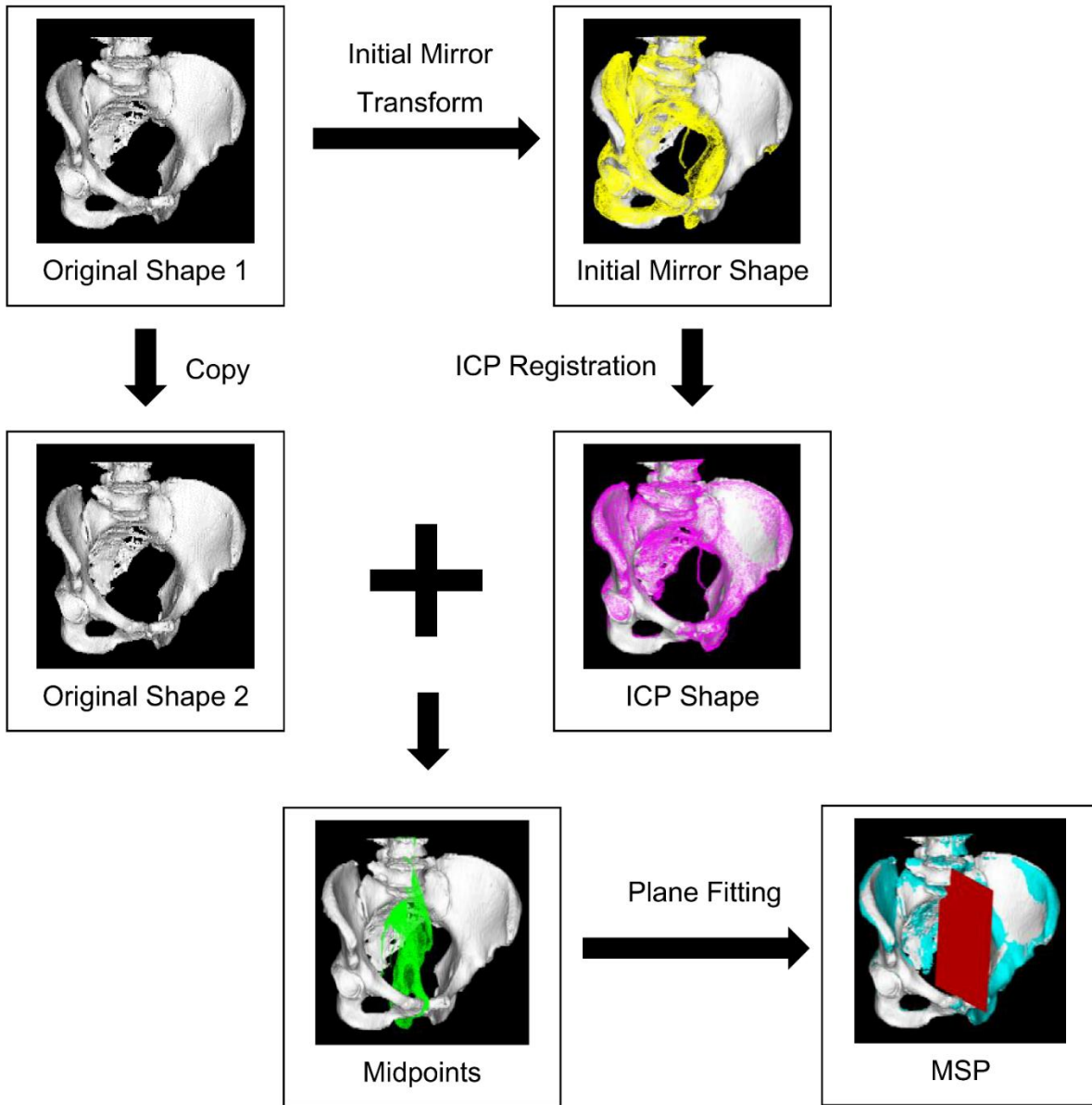
102 3. Select vertices near the markers using the spherical function in (1) (points outside of the sphere are removed).
 103 Traverse every point and compute their distance to the plane APP^k (n^k is the positive direction).

104 4. If the points with maximal distance to APP^k are not the same as markers M_i^k , go to step 2; else go to step 5.

105 5. Output the last plane APP^k and normal vector n^k to be the optimal APP solution.

106 **2.1.2 Midsagittal plane**

107 The MSP is computed as the mirror plane associated with approximately symmetrical structures in the pelvis. An
 108 initial estimate of the MSP passing through the midpoint between ASISs with a normal vector $(1,0,0)$ in the world
 109 coordinate system is used to mirror the original shape (Fig. 3).



110

111

Fig. 3. MSP computation pipeline.

112

113

Then, the initial mirror shape is registered with the original shape using the ICP algorithm. After iterative

computation, the optimal registration transform is

114

$$T_{opt} = T_{ICP} T_{IM}, \quad (2)$$

115

116

117

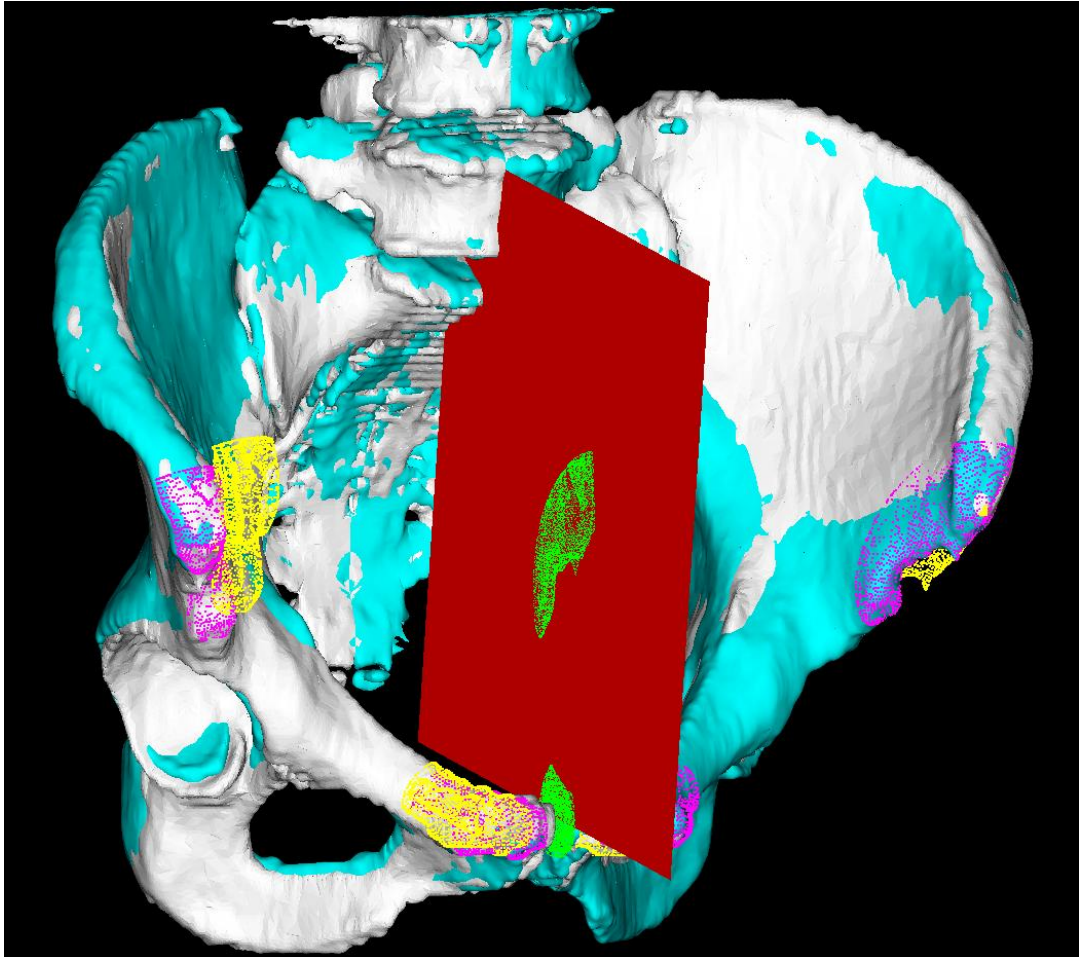
where T_{IM} is the initial mirror transform and T_{ICP} is the rigid ICP transform. However, T_{opt} is actually an affine

transform rather than the optimal mirror transform of the pelvis. Based on the order of surface points listed in the data,

each midpoint between the original position and the position after transform T_{opt} is calculated to form a midpoint set.

<

118 Because these points are all considered to be on the optimal mirror plane, a fitted least-squares plane (Fig. 4) should be the
119 MSP solution at the end of the computation.



120

121 Fig. 4. MSP computation process. The initial mirrored shape (yellow) is transformed to maximally fit the original shape (white) after ICP
122 registration. The midpoints (green) between corresponding points in the original shape and registered shape (purple) are used to fit a
123 least-squares MSP (red). Visualization of the optimal mirrored pelvis (indigo) after MSP modification indicates a good result.

124 From the clinical perspective, the ASISs and pubic tubercles could provide a reliable reference because they are
125 easily accessible when the patient is in the lateral position. However, from the graphical perspective, taking the entire
126 pelvis into account would provide a benefit, such as a more accurate estimate.

127 **2.1.3 The origin of the PCS and transverse plane**

128 Because the APP and MSP are computed without a perpendicularity constraint, it is necessary to modify one of
129 them to guarantee perpendicularity. We recommend modifying the MSP rather than the APP because the MSP has a higher
130 clinical significance. The normal vectors associated with the MSP and the APP provide the orientation of two coordinate
131 axes, and the orientation of the third coordinate axis is determined by a cross-product computation as

> REPLACE THIS LINE WITH YOUR PAPER IDENTIFICATION NUMBER (DOUBLE-CLICK HERE TO EDIT)

<

132
$$\mathbf{n}_{TPP} = \mathbf{n}_{MSP} \times \mathbf{n}_{APP}, \quad (3)$$

133 where \mathbf{n}_{APP} , \mathbf{n}_{MSP} , and \mathbf{n}_{TPP} are the normal vectors of the APP, MSP, and TPP, respectively. A guaranteed
 134 perpendicular MSP normal \mathbf{n}'_{MSP} is then computed from

135
$$\mathbf{n}'_{MSP} = \mathbf{n}_{APP} \times \mathbf{n}_{TPP}. \quad (4)$$

136 To compute the pelvic origin O_{PCS} , one of the markers on the APP is projected onto the MSP and then projected onto the
 137 TPP.

138 **2.2 Acetabular anatomy**

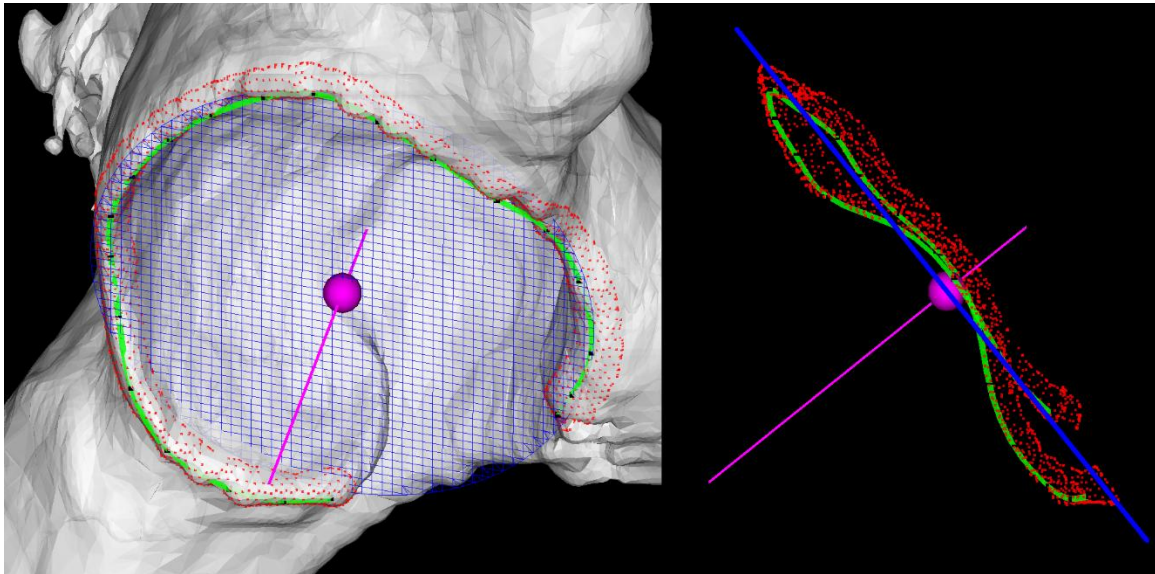
139 **2.2.1 Acetabular opening circle**

140 A recently published method introduced the use of a three-point circle as an initial estimate of the acetabular rim [24].
 141 However, the rim is usually not precisely circular. Our proposed method takes this into account. First, a series of nodes are
 142 manually located along the curved osseous ridge, and a cubic interpolation is used to build a B-spline path (Fig. 5). Then,
 143 surface points near the rim path are selected using a Boolean combination of spherical implicit functions. The clipping
 144 function that takes the minimum value of all implicit functions is

145
$$F = \min(F_1, F_2, \dots, F_n) \quad (5)$$

146 where F_i is a single spherical implicit function, as shown in (1), with its center at a point on the rim path and n is the
 147 number of rim points.

<



148

149 Fig. 5. Acetabular opening circle and axis determination. With about 20 nodes (black dots)
 150 manually located on the osseous ridge, a B-spline
 151 path (green) is built as the rim path using cubic
 152 interpolation. Points (red) on the surface model and near the rim path are collected to fit a
 least-squares spatial circle (blue grid). The center of rotation (purple sphere) and the normal axis of the opening plane (purple line) are
 computed.

153 These points on the rim represent many important anatomic parameters of the acetabulum, such as orientation, shape,
 154 and size. Spatial circle fitting is a convenient approach used to analyze the rim points. Here, we use a least-squares spatial
 155 circle, which is actually the intersection between a sphere and a plane that are separately fitted. Finally, the anatomic
 156 parameters of the acetabulum, such as those listed above (orientation, shape and size) can be easily computed from the
 157 acetabular opening circle in the PCS.

158 **2.2.2 Acetabular orientation in PCS**

159 Standard measures of anteversion and inclination of the acetabular axis have been introduced elsewhere [6]. The axis
 160 vector \mathbf{n}_a representing the acetabular orientation calculated by the plane fitting is in the image data coordinate system and
 161 the acetabular parameter calculation must be based on the standardized PCS, describing the orientation of the acetabulum
 162 in 3D space. For the illustration of the PCS, please refer to Fig. 3. in [25].

163 To determine these measures in the PCS, the acetabular axis should be transformed in advance as

$$164 \quad M_r = \begin{bmatrix} \mathbf{n}_{MSP} & \mathbf{n}_{APP} & \mathbf{n}_{TPP} \\ & & 1 \end{bmatrix}_{4 \times 4} \\ M_t = \begin{bmatrix} I & \mathbf{o}_{PCS} \\ & 1 \end{bmatrix}_{4 \times 4} \quad (6) \\ \mathbf{n}'_a = M_t M_r M_t^{-1} \mathbf{n}_a$$

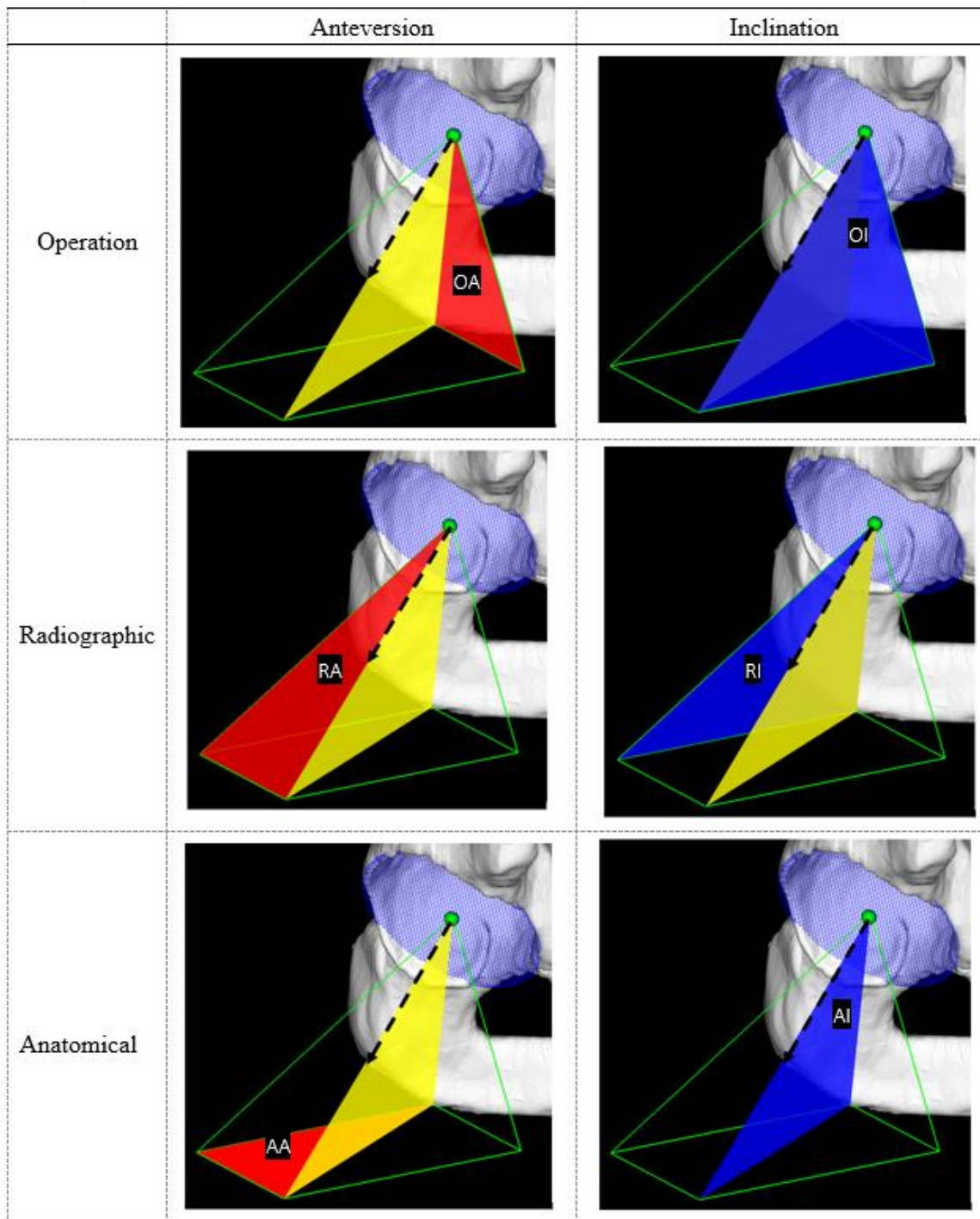
165 where M_r and M_t are the rotation and translation matrices about the PCS, respectively; \mathbf{n}'_a is the transformed direction

<

166 vector of the acetabular axis; and I is an identity matrix. With the normalized vector $\mathbf{n}'_a(x, y, z)$, the acetabular
 167 orientation parameters are computed as

$$\begin{aligned}
 & \begin{cases} \tan(OA) = y/z \\ \tan(OI) = |x|/\sqrt{y^2 + z^2} \end{cases} \\
 168 \quad & \begin{cases} \tan(RA) = -y/\sqrt{z^2 + x^2} \\ \tan(RI) = -|x|/z \end{cases} \\
 & \begin{cases} \tan(AA) = -y/|x| \\ \tan(AI) = -\sqrt{x^2 + y^2}/z \end{cases}
 \end{aligned} \tag{7}$$

169 where OA is operative anteversion; OI is operative inclination; RA is radiographic anteversion; RI is radiographic
 170 inclination; AA is anatomical anteversion; AI is anatomical inclination. (As shown in Fig 6., red represents anteverision
 171 and blue is inclination. The green arrow represents the acetabular axis.)



172

173

Fig. 6. Definition of the acetabular version

174

3. Experiment and evaluation

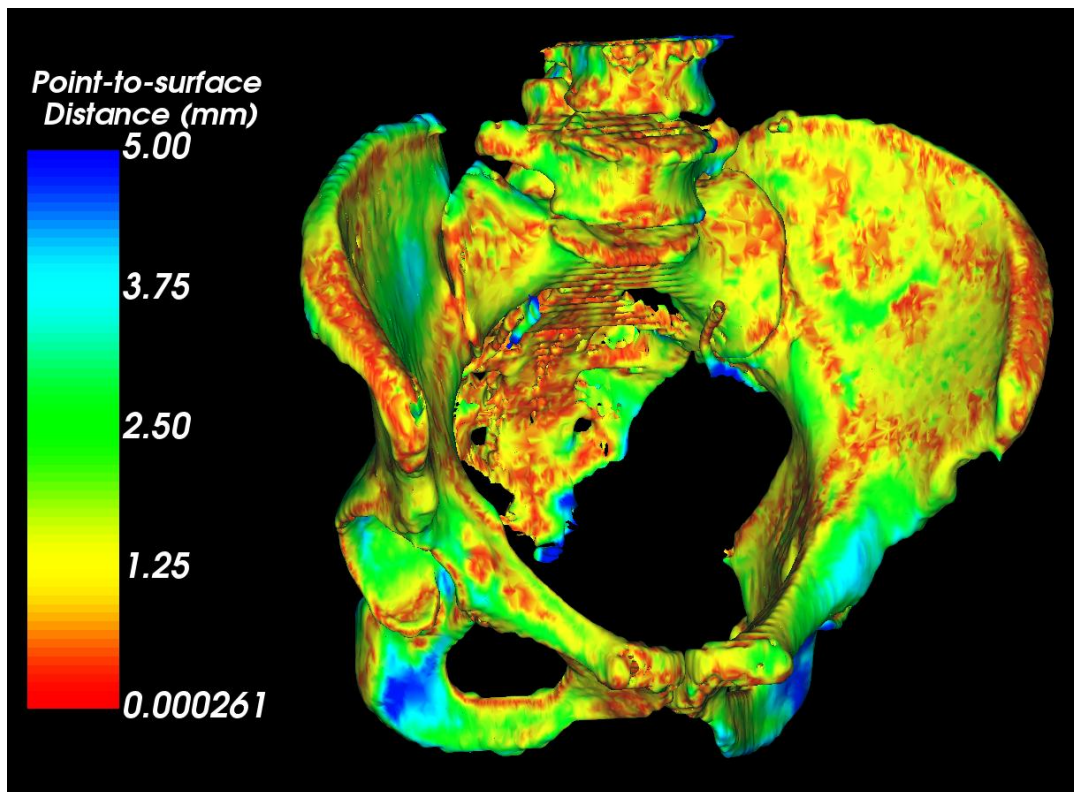
175 A 3D software package called “Acetabulometer”, was developed to execute the algorithm described above, and to

<

176 render the results of acetabular orientation. After importing the model, our proposed semi-automatic system can quickly
177 calculate the orientation.

178 For evaluation experiments, the right acetabulum was chosen. High-resolution CT data with a slice thickness of 1 mm
179 and an average in-plane (x-y) resolution of 0.977 mm of 88 normal people (mean age of 43 ± 27 years, 51 male and 37
180 female) receiving pelvic scans for reasons not related to orthopedic conditions were selected from Shanghai Nine
181 People's Hospital institution's database.

182 It is important to evaluate the accuracy of the APP and MSP computations. Theoretically, the APP is a unique
183 solution, and practically it can be obtained after at most four iterations. Rapid convergence required only one iteration in
184 60 cases (68.5%), two iterations in 21 cases (23.9%), three iterations in 5 cases (5.7%), and four iterations in 2 cases
185 (2.3%). The average number of iterations was 1.42 ± 0.33 , and the maximum was 4. Due to the complex 3D morphology
186 of the pelvis, evaluation of the MSP computation should also be surface-based. The point-to-surface distances between the
187 mirror pelvis and the original pelvis for every vertex of the model (Fig. 7) averaged over all 88 subjects was 1.34 ± 0.49
188 mm. As illustrated in Fig. 3, the ICP shape is the optimal mirror shape.



189

190

Fig. 7. Color-coded point-to-surface distances between the mirror pelvis and the original pelvis for every vertex.

<

191 This method performed well in the determination for all of the 88 subjects. The major error source from observers
 192 was the randomness of the placement of the initial markers, especially for the two endpoints of the rim path. Different
 193 observers placed the endpoints at different positions on the osseous ridge or in the notch. To evaluate the differences
 194 among raters and surface models, we produced three surface models of a random patient using different threshold values in
 195 segmentation, mesh smoothing, and decimation in reconstruction. Taking the parameter of the radiographic anteversion of
 196 acetabulum as an example, the experiment for the patient showed that values were similar across models and raters (Table
 197 1).

198 Table 1. Radiographic anteversion of acetabulum with different raters and surface models

Model \ Rater	Yiping Wang	Henghui Zhang	Liao Wang	SD
Surface Model 1	21.09°	21.52°	20.99°	0.23°
Surface Model 2	21.06°	21.04°	20.84°	0.099°
Surface Model 3	21.21°	20.69°	21.5°	0.33°
SD	0.065°	0.34°	0.28°	

199 Henghui Zhang and Liao Wang are clinical raters, while Yiping Wang is a technical rater.

200 The intra-class correlation coefficient (ICC) evaluation is a two-way analysis of variance model that accounts for
 201 random effects of both different users and subjects and it has been widely adopted to assess the reliability for a group of
 202 typical users [26]. In this study, ICC scores on anteversion and inclination in the standard angular definitions (operative,
 203 radiographic, and anatomic) and the radius of the acetabular rim were used to evaluate the reliability. Three trials were
 204 independently performed by three raters (Yiping Wang, Henghui Zhang, and Liao Wang) on all subjects. Raters started
 205 with raw DICOM (Digital Imaging and Communications in Medicine) images and performed all operations such as
 206 thresholding, segmentation, reconstruction, and initial marker placement using the 3D software. Both intra- (Table 2) and
 207 inter-rater (Table 3) ICC scores on these measures are high, indicating that the algorithms are very reliable and capable of
 208 accomplishing repetitive measurements for mass patient data.

209 Table 2. Single measure intra-rater reliability

Parameter \ Rater	Yiping Wang	Henghui Zhang	Liao Wang
Radius	0.9990 (0.9976 to 0.9996)	0.9893 (0.9755 to 0.9959)	0.9984 (0.9964 to 0.9994)
OA (operative anteversion)	0.9998 (0.9995 to 0.9999)	0.9986 (0.9968 to 0.9995)	0.9998 (0.9996 to 0.9999)
OI (operative inclination)	0.9989 (0.9975 to 0.9996)	0.9924 (0.9826 to 0.9971)	0.9988 (0.9972 to 0.9995)
RA (radiographic anteversion)	0.9998 (0.9996 to 0.9999)	0.9990 (0.9977 to 0.9996)	0.9998 (0.9996 to 0.9999)

RI (radiographic inclination)	0.9981 (0.9957 to 0.9993)	0.9893 (0.9756 to 0.9959)	0.9987 (0.9970 to 0.9995)
AA (anatomical anteversion)	0.9998 (0.9996 to 0.9999)	0.9989 (0.9976 to 0.9996)	0.9998 (0.9995 to 0.9999)
AI (anatomical inclination)	0.9985 (0.9966 to 0.9994)	0.9910 (0.9794 to 0.9966)	0.9990 (0.9976 to 0.9996)

210 The values are given as the intra-rater ICC scores, with the 95% confidence interval in parentheses, for single measures in
 211 terms of absolute agreement (an ICC of approximately 0.90 to 1.00 for Cronbach alpha can be considered almost perfect).

212

213

Table 3. Single measure inter-rater reliability

Parameter	Trial	Trial 1	Trial 2	Trial 3
Radius		0.9981 (0.9956 to 0.9993)	0.9988 (0.9757 to 0.9994)	0.9985 (0.9965 to 0.9994)
OA (operative anteversion)		0.9997 (0.9992 to 0.9999)	0.9998 (0.9990 to 0.9999)	0.9997 (0.9996 to 0.9999)
OI (operative inclination)		0.9979 (0.9952 to 0.9992)	0.9974 (0.9969 to 0.9991)	0.9982 (0.9978 to 0.9995)
RA (radiographic anteversion)		0.9998 (0.9995 to 0.9999)	0.9998 (0.9997 to 0.9999)	0.9998 (0.9996 to 0.9999)
RI (radiographic inclination)		0.9966 (0.9921 to 0.9987)	0.9963 (0.9956 to 0.9973)	0.9977 (0.9970 to 0.9987)
AA (anatomical anteversion)		0.9997 (0.9994 to 0.9999)	0.9999 (0.9998 to 0.9999)	0.9998 (0.9996 to 0.9999)
AI (anatomical inclination)		0.9973 (0.9938 to 0.9990)	0.9980 (0.9977 to 0.9985)	0.9978 (0.9956 to 0.9986)

214 The values are given as the inter-rater ICC scores, with the 95% confidence interval in parentheses, for single measures in
 215 terms of absolute agreement (an ICC of approximately 0.90 to 1.00 for Cronbach alpha can be considered almost perfect).

216

217

4. Discussion and conclusion

218 We have presented a novel surface-based approach to determine key spatial parameters of the acetabulum. A new
 219 PCS consisting of the APP, MSP, and TPP was derived from a 3D pelvic surface model. Based on the PCS, critical
 220 acetabular parameters can be determined semi-automatically. High efficiency was achieved for the entire algorithm
 221 procedure while enabling highly reproducible measurements of acetabular spatial parameters, with almost perfect inter-
 222 and intra-rater ICC scores.

223 Compared with the MSP determination using simple landmark points, the surface-based approach maximally reduces
 224 manual error of acetabular angle measurements and greatly improves the reliability. The computation time depends on the
 225 number of points on the surface model and the number of iterations in the ICP algorithm. In this study, we chose at most
 226 50 iterations as adequate and 0.001 mm as the maximum mean distance. The number of vertices on each pelvis model was
 227 about 300,000. The time consumption was less than 2 seconds after selection of the four initial points for each case using a
 228 standard PC, which is comparable with the study reported by Fieten *et al.* [22].

<

229 A better description of the acetabulum should be a spatial circle. Different investigators have taken different
230 approaches to modeling acetabular orientation. Higgins *et al.* [24] presented a best-fit plane for describing the acetabular
231 orientation. Jóźwiak *et al.* [27] presented a set of section planes parallel to the acetabular opening plane to search for an
232 average trend line that joins the centers of the circles fitted by the intersection curve. We took the point set on the
233 acetabular rim as a feature extraction and found that an acetabular circle could provide a succinct description, which helps
234 to determine the center of rotation. A circle with its radius, perimeter, and normal vector can be computed by combining
235 sphere-fitting and plane-fitting algorithms. An average point-to-circle error of 3.03 millimeters was obtained in the circle
236 fitting experiments. However, the main error source is not computational, but rather the complex morphology of the native
237 acetabulum. A better description of every native acetabulum may be an equation of a best-fit curve in a cylindrical
238 coordinate system. Related work is in progress, and we believe that it is meaningful not only for pre-planning and
239 image-guidance of THA interventions, but also for patient-specific design of acetabular prostheses in the future.

240 Optimal placement of the acetabular prosthesis is critical for the success of THA. However, the target placement for
241 the prosthetic component is still unknown. The current measurement of the native acetabulum as well as the acetabular
242 component is not accurate or reliable without taking the pelvis into account. Our “Acetabulometer” establishes a reliable
243 3D PCS and measures the critical acetabular parameters based on the reported PCS. Overall, the semi-automated
244 segmentation and measurement system is sufficiently fast, accurate, and reliable to be applied to the analysis of a large
245 sample. Our approach may have the potential to determine the optimal target for the placement of the acetabular
246 component in THA.

247

248 **Conflict of interests**

249 None declared.

250

251 **Funding**

252 This study was supported by the Foundation of Science and Technology Commission of Shanghai Municipality

<

253 (15510722200, 16441908400), Shanghai Jiao Tong University Foundation on Medical and Technological Joint Science
 254 Research (YG2016ZD01, YG2015MS26), The Royal Society International Exchanges scheme (IE140967, IE141258), and
 255 the EPSRC UK Image-Guided Therapies Network+ (EP/N027078/1) and EPSRC-NIHR HTC Partnership Award 'Plus':
 256 Medical Image Analysis Network (EP/N026993/1).

257 **Ethical approval**

258 Not required.

References

259 [1] Kurtz S, Ong K, Lau E, Mowat F, Halpern M. Projections of primary and revision hip and knee arthroplasty in the United States from. *Journal of Bone &*
 260 *Joint Surgery*. 2007;89:780-5.

261 [2] Beckmann J, Lüring C, Tingart M, Anders S, Grifka J, Köck FX. Cup positioning in THA: Current status and pitfalls. A systematic evaluation of the literature. *Archives of Orthopaedic & Trauma Surgery*. 2009;129:863-72.

262 [3] Lewinnek GE, Lewis JL, Tarr R, Compere CL, Zimmerman JR. Dislocations after total hip-replacement arthroplasties. *Journal of Bone & Joint Surgery American Volume*. 1978;60:217-20.

263 [4] Archbold HA, Mockford B, Molloy D, Mcconway J, Ogonda L, Beverland D. The transverse acetabular ligament: an aid to orientation of the acetabular component during primary total hip replacement: a preliminary study of 1000 cases investigating postoperative stability. *Journal of Bone & Joint Surgery British Volume*. 2006;88:883-6.

264 [5] Murray DW. The definition and measurement of acetabular orientation. *Journal of Bone & Joint Surgery British Volume*. 1993;75:228-32.

265 [6] Maruyama M, Feinberg JR, Capello WN, D'Antonio JA. Morphologic features of the acetabulum and femur: anteversion angle and implant positioning. *Clinical Orthopaedics & Related Research*. 2001;393:52-65.

266 [7] Chu C, Bai J, Wu X, Zheng G. MASCG: Multi-Atlas Segmentation Constrained Graph method for accurate segmentation of hip CT images. *Medical image analysis*. 2015;26:173-84.

267 [8] Yokota F, Okada T, Takao M, Sugano N, Tada Y, Tomiyama N, et al. Automated CT segmentation of diseased hip using hierarchical and conditional statistical shape models. *Medical Image Computing & Computer-assisted Intervention: Miccai International Conference on Medical Image Computing & Computer-assisted Intervention2013*. p. 190-7.

268 [9] Ellingsen LM, Chintalapani G. Robust deformable image registration using prior shape information for atlas to patient registration. *Computerized Medical Imaging & Graphics the Official Journal of the Computerized Medical Imaging Society*. 2009;34:79-90.

269 [10] Lubovsky O, Peleg E, Joskowicz L, Liebergall M, Khouri A. Acetabular orientation variability and symmetry based on CT scans of adults. *International Journal of Computer Assisted Radiology & Surgery*. 2010;5:449-54.

270 [11] Stem ES, O'Connor MI, Kransdorf MJ, Crook J. Computed tomography analysis of acetabular anteversion and abduction. *Skeletal Radiology*. 2006;35:385-9.

271 [12] Ghelman B, Kepler CK, Lyman S, Valle AGD. CT outperforms radiography for determination of acetabular cup version after THA. *Clinical Orthopaedics & Related Research*. 2009;467:2362-70.

272 [13] Klaue K, Wallin A, Ganz R. CT evaluation of coverage and congruency of the hip prior to osteotomy. *Clinical Orthopaedics & Related Research*. 1988;232:15-25.

273 [14] Rittmeister M, Callitsis C. Factors influencing cup orientation in 500 consecutive total hip replacements. *Clinical Orthopaedics & Related Research*. 2006;445:192-6.

274 [15] Murtha PE, Hafez MA, Jaramaz B. Variations in acetabular anatomy with reference to total hip replacement. *Bone & Joint Journal*. 2008;90:308-13.

275 [16] Dandachli W, Islam SU, Tippett R, Hall-Crags MA, Witt JD. Analysis of acetabular version in the native hip: comparison between 2D axial CT and 3D CT measurements. *Skeletal Radiology*. 2011;40:877-83.

276 [17] Puls M, Ecker TM, Steppacher SD, Tannast M, Siebenrock KA, Kowal JH. Automated detection of the osseous acetabular rim using three-dimensional models of the pelvis. *Computers in Biology & Medicine*. 2011;41:285-91.

277 [18] Foroughi P, Song D, Chintalapani G, Taylor RH, Fichtinger G. Localization of Pelvic Anatomical Coordinate System Using US/Atlas Registration for Total Hip Replacement. *Medical Image Computing & Computer-assisted Intervention: Miccai International Conference on Medical Image Computing & Computer-assisted Intervention2008*. p. 871-9.

278 [19] Cerveri P, Marchente M, Chemello C, Confalonieri N, Manzotti A, Baroni G. Advanced computational framework for the automatic analysis of the acetabular morphology from the pelvic bone surface for hip arthroplasty applications. *Annals of biomedical engineering*. 2011;39:2791-806.

279 [20] Nikou C, Jaramaz B, Digioia AM, Levison TJ. Description of Anatomic Coordinate Systems and Rationale for Use in an Image-Guided Total Hip Replacement System. *International Conference on Medical Image Computing and Computer-Assisted Intervention2000*. p. 1188-94.

280 [21] Wu G, Siegler S, Allard P, Kirtley C, Leardini A, Rosenbaum D, et al. ISB recommendation on definitions of joint coordinate system of various joints for the reporting of human joint motion—part I: ankle, hip, and spine. *Journal of biomechanics*. 2002;35:543-8.

281 [22] Fieten L. Surface-based determination of the pelvic coordinate system. *Proceedings of SPIE - The International Society for Optical Engineering*. 2009;7261:726138---10.

282 [23] Fieten L, Eschweiler J, Fuente MDL, Gravius S, Radermacher K. Automatic extraction of the mid-sagittal plane using an ICP variant. *Medical Imaging2008*. p. 69180L-L-11.

306 [24] Higgins SW, Spratley EM, Boe RA, Hayes CW, Jiranek WA, Wayne JS. A novel approach for determining three-dimensional acetabular orientation: results
307 from two hundred subjects. *Journal of Bone & Joint Surgery*. 2014;96:1776-84.

308 [25] Zhang H, Wang Y, Ai S, Chen X, Wang L, Dai K. Three-dimensional acetabular orientation measurement in a reliable coordinate system among one
309 hundred Chinese. *Plos One*. 2017;12:e0172297.

310 [26] Bonett DG. Sample size requirements for estimating intraclass correlations with desired precision. *Statistics in Medicine*. 2002;21:1331-5.

311 [27] Jozwiak M, Rychlik M, Musielak B, Chen BP, Idzior M, Grzegorzewski A. An accurate method of radiological assessment of acetabular volume and
312 orientation in computed tomography reconstruction. *BMC Musculoskeletal Disorders*. 2015;16:42.